LV CONTOUR TRACKING IN MRI SEQUENCES BASED ON THE GENERALIZED FUZZY GVF

Wufan Chen [1] *Shoujun Zhou* [2] *Bin Liang* [3]

1. Key Lab for MIP, the First Military Medical Univ., G. Z. (510515), China. chenwf @fimmu.edu.cn
2. Key Lab for MIP, the First Military Medical Univ., G. Z. (510515), China. shoujun@fimmu.edu.cn
3. Guang Dong Branch of NSBC, S & T Zone, G. Z. (510515), China. lb@gd_mail.nisac.gov.cn

ABSTRACT

For the segmentation and robust tracking of the cardiac left ventricle (LV) in MRI sequences, an optimized algorithm is presented in this paper, which is based on the active contour framework. To use the active contours model (ACM [1]) estimating the cardiac motion, a new concept of generalized fuzzy gradient vector flow (GFGVF) is presented and compared with the classical gradient vector flow (GVF [2,3]). Then a modified ACM is proposed for motion tracking, which is based on two new external forces: one is the GFGVF field; the other is the relativity of optical flow field (OFF) on predictive contour. For robust tracking the outline of interest, a set of motion equations is presented to describe two correlative updating steps. Another, given some prior terms and likelihood one, the motion state of each point can be found by the Maximum a Posteriori Probability (MAP).

1. INTRODUCTION

In this paper, a particular tracking method, based on optimized external fields, is presented for the periodic non-rigid motion of endocardiac boundary in cardiac image sequences (CIS).

As an important analysis method, ACM [1] has a fundamental property: If it is used to segment an image or search the region of interest (ROI) in images, ACM can stably settle at the object region and come into being a close chain code under the action of some internal and external forces. This is challenging because the artifacts in CIS and elements of clutter around the contours may mimic parts of contour features. In the most severe case of camouflage, the clutter may consist of objects similar to the contour object.

Chenyang Xu and Jerry L.[2] present a GVF field and use it as new external force term to constraint snake in images. Up to now, the GVF field has dominated over many external force fields for its greater active range and approaching to the boundary concavity regions of image. But then, for the CIS comprising much clutter, the classical GVF field is often abnormal when the vectors flows around the weak boundaries tend to be absorbed by strong one, so the true ROI edge around dark boundaries in images is neglected. How to avoid the adverse conditions is to be concerned.

Accordingly, some better algorithms are proposed for the non-rigid tracking in this paper: First of all, the generalized fuzzy operator (GFO) [3] is adopted to optimize the GVF, by which a generalized fuzzy gradient vector (GFGVF), as the external force, comes into being. For tracking model, a set of modified snake equations is presented, which is based on the GFGVF and other two external forces of the optical flow and a modified relativity of predictive contour [4].

Considering the background of this paper, the typical computing equations of external force and the energy function of snake are quoted as follows:

By the property of image's gradient and 2D Gauss function, the typical external force is expressed as:

$$\nabla E^2{}_{ext}(x,y) = \left|\nabla(G_\sigma(x,y) * I(x,y))\right|^2 \qquad (1)$$

Normally, the formula above can only acquire lesser dynamic range. To improve it, the algorithm developed from expression (1) is the GVF diffusion equation, and denoted by:

$$\mathrm{u}_t = \eta\nabla^2 \mathrm{U} - |\nabla I|^2\ (\mathrm{U} - \nabla I)^2 \qquad (2)$$

where the constant η and the normal gradient $|\nabla I|^2$ act as weighing functions of smoothing item and data item respectively. Then, the gradient vector flow $U(x,y)$ can be solved exactly by iteration technique.

During tracking the edge of ROI in 2D image, the contour is expressed as $P(s) = [x(s), y(s)]$ where $s \in [0,1]$. The deformation of ACM is controlled by the minimum energy function of snake as follows:

$$E = \int_0^1 [\alpha |P'(s)|^2 + \beta |P''(s)|^2 + E_{ext}(P(s))]ds \qquad (3)$$

where α and β are the elasticity coefficient and rigidity one, respectively.

In addition, to acquire the point-wise motion state, spatial coherence and temporal continuity terms (SCTC) are introduced in the MAP algorithm to restrict the sampling and updating. Thus it can be seen that a complete algorithm for robust tracking of CIS comes into being.

2. GENERALIZED FUZZY GRADIENT VECTOR FLOW

To compute the GFGVF, the concept of generalized fuzzy set (GFS) should be given as follows:

Definition 1. Denoting GFS F on region U as:

$$F = \{\mu_F(x),\ \ x \in U\} \qquad (4)$$

where $\mu_F(x) \in [-1,1]$ is called the GF membership function (GMF) of F on U; $\mu_F(x) \in [-1,0)$, GMF of x non-subordinate to F on U; $\mu_F(x) \in (0,1]$, GMF of x subordinate to F on U; $\mu_F(x) = 0$, the fuzzy bound point function (FBF) of F on U.

When a cardiac image I is regarded as a finite field consisting of finite elements, $I = \{x_1, x_2, ..., x_n\}$ where x_i is

This work was supported by "973" program of China (No. 2002CB312104), Key NNSF of China (No.30130180), and NNSF of China (No.60302022).

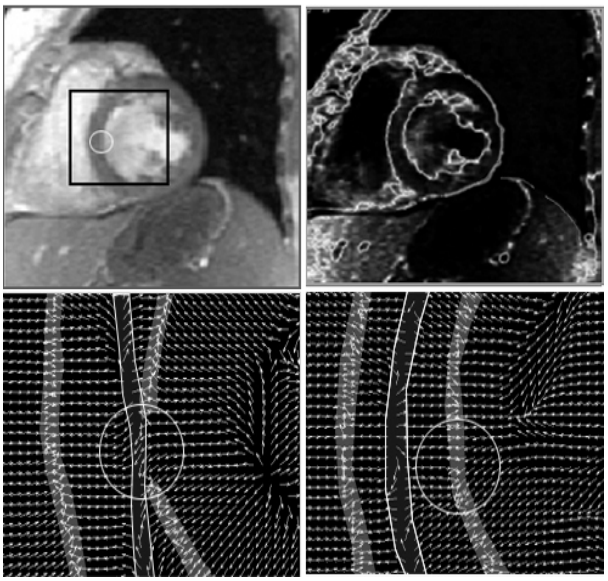

Fig.1 Comparison between GVF and GFGVF: (a) Left-upside, MR cardiac image; (b) Right-upside, GF edge detection; (c) Left-downside, the GVF field; (d) Right-downside, the GFGVF field.

the grey level of pixel i, the GFS set of I can be defined as the fuzzy set on finite field *I* and written as:

$$F = \mu_F(x_1)/x_1 + ... + \mu_F(x_n)/x_n = \bigcup_{i=1}^{n} \mu_F(x_i)/x_i \qquad (5)$$

To compute the GMF, we can expressed the function $\mu_F(\cdot)$ above as: $\mu_{\mathrm{F}}(x_i) = \cos(\pi \cdot \frac{x_{\max} - x_i}{x_{\max} - x_{\min}})$.

If $\gamma = \mu_{\mathrm{X}}(\xi) \cong 0$ denotes the FBF of F on I, the GFO can be defined as follows:

Definition 2. A normal fuzzy set F'=[0,1] can be produced when GFO acts on the set of the GFM of *F*. Then the generalized fuzzy transform can be written as:

$$\mu'_F(x)] = \begin{cases} \sqrt{1-[1+\mu_F(x)]^2}, & -1 \le \mu_F < 0 \\ [\mu_F(x)]^2, & 0 < \mu_F \le r \\ \sqrt{1-0.5[1-\mu_F(x)]^2}, & r < \mu_F \le 1 \end{cases} \qquad (6)$$

The processed cardiac image is displayed in Fig1. (b).

Integrating with the definitions above, the Eq.(2) can be modified as follow. Firstly, we can let:

$$g(\cdot) = \eta \exp[-(|\mu'_F|/\sigma)^2],\ h(\cdot) = \rho[1-g(\cdot)]|\nabla I|^2 \qquad (7)$$

where $g(\cdot)$ and $h(\cdot)$ are the functions of monotonously decreasing and monotonously increasing respectively, η is the smoothness level and σ corresponds to standard variance used to control the dynamic value. Secondly, substituting (7) into (2) to control the iterative process, the GFGVF diffusion equation is expressed as:

$$\mathrm{u}_t = g(|\mu'_F|)\nabla^2 \mathrm{U} - \rho(1-g(\mu'_F))|\nabla I|^2\ (\mathrm{U}-\nabla I)^2 \qquad (8)$$

The GFGVF field of an edge image detected by GFO has such properties: in location where the change of gray lever slow down, the value of $g(\cdot)$ will increase and the value of $h(\cdot)$ will decrease, thus the smoothness action is more effective and the gradient variation is lesser; vice versa.

Comparing with GVF, the main difference between them is that the smoothing term and data term of the GFGVF are formed by generalized fuzzy edge information, which can ensure that the GFGVF not only has the same dynamic range as that of the GVF but also has better boundary controllability. The characteristic above can be displayed in Fig.1(c) and Fig.1(d).

3. ROBUST TRACKING OF ACTIVE CONTOUR

When the evolution of contour is regarded as two steps: the deformation inside frame and interval shift between sequential frames, the corresponding two external forces can be denoted respectively by:

$$F_1^{ext} = |F_{ext}^{img}| \cdot \widetilde{F}_{ext}^{img} \qquad (8)$$

$$F_2^{ext} = |F_{ext}^{img}| \cdot (\widetilde{F}_{ext}^{opt} + \widetilde{F}_{ext}^{img}) \qquad (9)$$

where $\widetilde{F}_{ext}^{img}$ is the GFGVF, $\widetilde{F}_{ext}^{opt}$ is the optical flow, and formula (9) expresses a composite force.

Next, a set of equations can be presented for the active contour tracking. Two snake equations are formulated here, one is the static and used for internal updating of a frame, and the other is the dynamic and used for interval updating between frames; about their formation; the static one corresponds with the classic one, while the dynamic one can be denoted by:

$$\min \int_0^1 \tfrac{1}{2}[\alpha |P'(s)|^2 + \beta |P''(s)|^2] + W(P(s),C(s))E_{ext}(P(s))ds \qquad (10)$$

where $P(s)$ is the contour of current frame and $C(s)$ is the predictive one of next frame. We use the weighting function $W(P(s),C(s))$ to restrict the motion amplitude resulted from the external force $E_{ext}(P(s))$. Based on the conventional algorithm of optical flow $\widetilde{F}_{ext}^{opt}(u(x,y),\ v(x,y))$, the relativity can be expressed as:

$$\begin{aligned}(\Delta\hat{\mathrm{x}}, \Delta\hat{\mathrm{y}}) &= \min_{(\Delta x, \Delta y) \in N_s} E(f_p, f_c) \\ &= \min_{(\Delta x, \Delta y) \in N_s} \textstyle\sum_{N_s} [(u_P - u_C)^2 + (v_P - v_C)^2]\end{aligned} \qquad (11)$$

where N_s is a searching window, f_P, f_C are respectively the optical flow vector distributed on the contour of the current frame and the one distributed on the predictive contour of the next frame; the variable $\Delta\hat{x}, \Delta\hat{y} \in (-N_s/2,\ N_s/2)$ are the variation from the center of window N_s. The expression $E(f_p, f_c)$, as a new predictive contour inertia energy term, can measure the variation between $P(s)$ and $C(s)$. Then the function $W(P(s),C(s))$ can be expressed as:

$$W(P(s),C(s)) = 1 + (\Delta\hat{x} + \Delta\hat{y})/N_s \qquad (12)$$

Obviously, the value of W is normalized to the range $[0,1]$. Consequently, the iterative amplitude $W(Y_p, \hat{Y}_c)F_2^{ext}$ in the following equation (13.4) can adaptively control the rate of snake approaching the object from current frame to next one. Let $X(n) = (X_1(n), X_2(n), \cdots X_M(n))$ and $Y(n) = (Y_1(n), Y_2(n), \cdots Y_M(n))$, where X is the space coordinate vector of the chain code in a single frame and Y is the one in interval frame. Refer to principle of the finite difference, A set of

sequentially updating equations about motion tracking of active contours can be written as:

$$\begin{aligned}
&1)\quad X^0(n)=\hat{Y}(n);\\
&2)\quad X^{k+1}(n)=(I-\gamma A)^{-1}[\gamma X^k(n)+F_1^{ext}(X^k(n))];\\
&3)\quad Y^0(n+1)=X(n);\\
&4)\quad \hat{Y}^{k+1}(n+1)=(I-\gamma A)^{-1}[\gamma Y^k(n+1)\\
&\qquad\qquad +W(Y_p^n,\hat{Y}_c^{n+1})F_2^{ext}(Y^k(n+1))];
\end{aligned}\tag{13}$$

where A, the coefficient matrix with size $M\times M$, contains the parameter item $\alpha\,\&\,\beta$, n is the frame number and k is iteration number, and γ is the viscosity parameter. The meaning of equations (13) can be described as: Firstly, the original active contour $\hat{Y}(n)$ has been provided by the result in the nth frame or hand sketching in the first frame. The vector $X(n)$, as the real contour in the nth frame, can be calculated by the iterated equation (13.2). In succession, the vector $\hat{Y}(n+1)$, as an estimated contour in the n+1th frame, can be computed by the iterated Eq. (13.4). For the calculated $\hat{Y}(n+1)$ approaching to the true outline of the n+1th frame, equations (13.1) and (13.2) are again used. At last the exact contour $X(n+1)$ of the n+1th frame can be worked out.

4. DELINEATION OF POINT'S MOTION TRAJECTORIES

After the process above being completed, the chain code $P_n(s)$ can be acquired. Then, the point's tracking algorithm of MAP can be implemented. Let $\{S_n(x_i,y_i)\mid i=1,\cdots,M\}$ denote the position of M entries of points in the kth frame, and index i have a nonlinear corresponding relation to s. Under the known position of snake and some priori term, the MAP estimation of $\widehat{S}_n$ can be described as:

$$\widehat{S}_n=\arg\max_{(x,y)\in F}\{p(S_n)p(P_n\mid S_n)\}\tag{14}$$

If the motion being regarded as the Markov random field, the moving particles of the non-rigid object satisfy the independence requirement. Another, the points adjacent to the contour satisfy the motion-space coherence; similarly, for the cardiac keeps a periodic motion, each point satisfies temporal continuity in some extent. The characteristic above can be illustrated in Fig.2. If the optical flow vector of the point m in contour of the nth frame can be denoted by $V_n(m)$, the motion space coherence and point temporal continuity (SCTC) can be expressed as follows:

$$P(S_n)=\frac{\exp[-(\frac{1}{2})(\widetilde{V}_n(i)-V_n(i))'K_L^{-1}(\widetilde{V}_n(i)-V_n(i))]}{\sqrt{(2\pi)^3K_L}}\cdot\frac{\exp[-(\frac{1}{2})(V_{n+1}(i)-V_n(i))'K_R^{-1}(V_{n+1}(i)-V_n(i))]}{\sqrt{(2\pi)^3K_R}}\tag{15}$$

Given the chain code $P_n(s)$ of contour in the nth frame, when the points move from the position S_{n-1} to S_n, the probability $p(P_n\mid S_n)$ in Eq.(14) denotes the variation relative to the chain code P^n, as the likelihood term, can be written as:

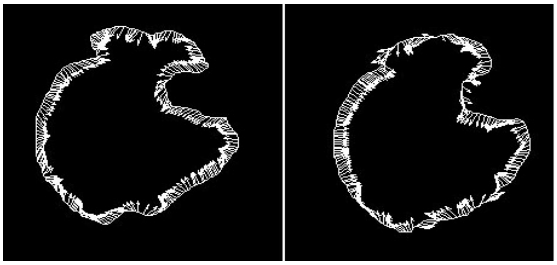

(a) (b)

Fig.2 SCTC about the contour of cardiac left ventricular: (a) the current contour and its motion direction; (b) the next contour and its motion direction.

$$p(P_n\mid S_n)=\frac{\exp[-(\frac{1}{2})(P_n(i)-S_n(i))'K_C^{-1}(P_n(i)-S_n(i))]}{\sqrt{(2\pi)^3K_C}}\tag{16}$$

Computed by Eq.(14), the motion trajectories of the points on the initial contour can be acquired. The point's trajectories in half cycle are displayed in Fig.4(a), where the SCTC can also be displayed effectively.

5. EXPERIMENTAL RESULTS AND CONCLUSION

In this experiment, two sequences of CIS_1 and CIS_2 are used for tracking the cardiac left ventricular (LV). Lots of comparisons have been made based on the difference between: (A) classical edge detection operator and GFO; (B) the GVF diffusion equation and the GFGVF one; (C) the classical ACM tracking model [1] and the modified one. The calculated results indicate that the latter one of each item above has better effect than the preceding one. To display the principal difference, Fig.3 describes the different results of deformation and tracking (RDT) under GVF and GFGVF respectively. Apparently, the results of underside in Fig.3 are better than that of upside, which not only illuminate the validity and robustness of the modified model but also indicate the better segmentation effect based on the GFGVF than that based on the GVF.

After the active contour in CIS is iteratively solved, each point in the contours of CIS_1 is tracked by the MAP algorithm and displayed in Fig.4 (a). In Fig.4 (b), considering the motion amplitude of twelve feature points during a period (22 frames) of movement, not all the points return to the initial position, and only up to 80 percent of points come back to the position less then 4 pixels from the initial one. By analysis, the reason is that the 2D images can only approximately reflect the 3D non-rigid motion. In cardiac clinic diagnosis, this method can be used to detect many symptoms.

Given the function $e(t)=\sqrt{\frac{1}{M_n}\sum_{m=1}^{M_n}(\hat{P}_m(t)-\overline{P}_m(t))^2}$

where M_n is the normalized contour length, $\overline{P}_m$ and $\hat{P}_m$ denote the normal contour and the estimated one respectively, the results of mean square quantization error (MSQR) in CIS_1 and CIS_2 are respectively displayed in Tab.1 and Tab.2.

MSQR	$e(1)$	$e(3)$	$e(5)$	$e(7)$	$e(9)$	…	$\overline{e}(n)$
GFGVF	1.2843	1.4219	2.3216	0.8560	2.7624	…	2.336
GVF	2.3607	3.4138	4.1320	1.3330	5.7330	…	4.210

Tab. 1 MSQR of contour tracking in CIS_1

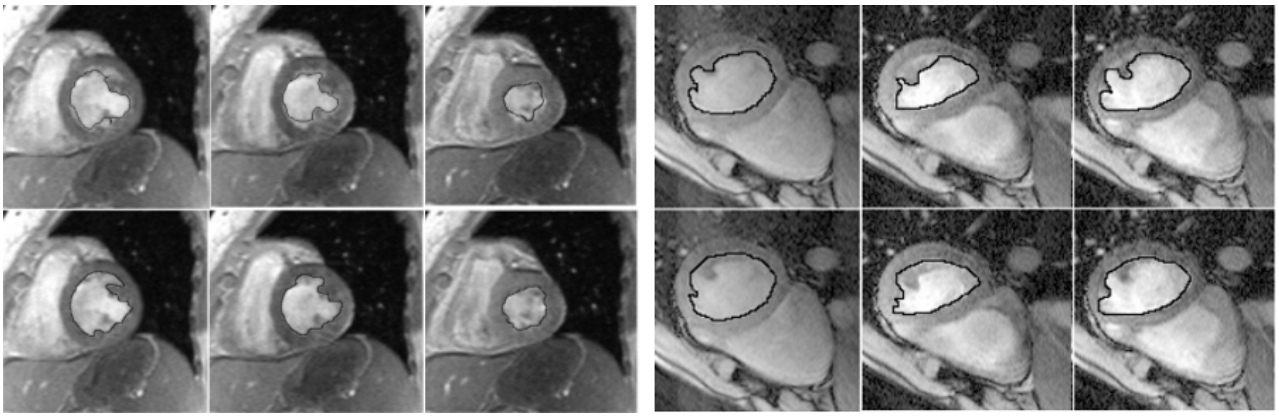

No.1 Fr., CIS_1 No. 3 Fr., CIS_1 No. 9 Fr., CIS_1 No. 1 Fr., CIS_2 No. 9 Fr., CIS_2 No. 11 Fr., CIS_2

Fig.3 Comparison of the contour tracking based on the two external force fields. Upside: the RDT by the external force of GVF; Underside: RDT by the external force GFGVF.

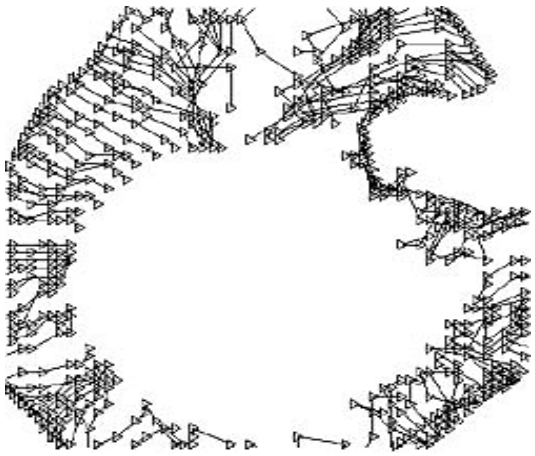

Fig. 4 The partial trajectories of points in the LV wall

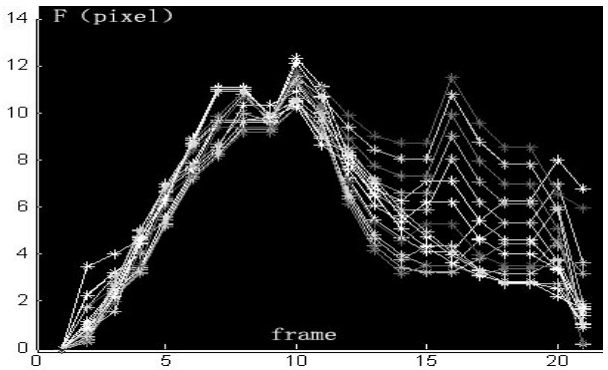

Fig.5 The motion amplitude of several feature points.

MSQR	$e(1)$	$e(3)$	$e(5)$	$e(7)$	$e(9)$	…	$\bar{e}(n)$
GFGVF	1.2451	1.4334	0.8135	1.3390	1.1240	…	1.3012
GVF	4.3245	5.3002	1.0234	1.5460	6.1032	…	5.0341

Tab. 1 MSQR of contour tracking in CIS_2

Summarily, the better method of contour tracking and point-wise estimation about the cardiac non-rigid motion is presented in this paper. The method above is based on the robust external field of GFGVF, which is very useful for the application of tracking medical non-rigid motion. The operation process is composed by two steps of tracking phase, respectively used to solve the problems of the deformation inside a frame and estimation in interval frames. The method has been validated by comparing the manually outlined edges with the results of tracking. For that the classical GVF field and OFF have been formed in 3-D space [2, 5], this system which based on the 2-D GFGVF field can be expanded to 3-D. Therefore, the system establishes a framework from which a system for 3-D tracking can be constructed.

REFERENCES

[1] M. Kass, A. Wikin, and D. Terzopaulos, "Snakes: active contour modes", Int.J.Comput.Vision, 1: 321-331, 1998.

[2] Chenyang Xu and Jerry L. Prince, Gradient Vector Flow Deformable Models, Academic Press, Sep, 2000.

[3] Chung-Chu Leung and Wufan Chen, "Brain Tumor Boundary Detection in MR Image with Generalized Fuzzy Operator", IEEE ICIP Conference in Barcelona Spain, Sep.14-17, 2003.

[4] Hao Jiang and Mark S. Drew, "A predictive contour inertia snake model for general video tracking", IEEE ICIP Sep. 22-25, 2002.

[5] J. Barron and H. Spies, "Quantitative regularized range flow", Vision Interface, VI, 2000.

[6] J. Vermaak, P. Pérez, M. Gangnet, and A. Blake. "Towards improved observation models for visual tracking: selective adaptation", Eur. Conf. on Computer Vision, ECCV'2002, Copenhagen, Denmark, June 2002.

[7] Yunqiang Chen and Thomas S. Huang, **"**Optimal radial contour tracking by dynamic programming", Proc. of IEEE ICIP 2001, Thessaloniki, Greece, October 2001.

[8] Ivana Mikic, Slawomir Krucinski and James D.Thomas, "Segmentation and Tracking in Echocardiographic Sequences: Active Contours Guided by Optical Flow Estimates", IEEE *transactions on medical imaging*, Vol.17, No. 2 pp.127-136, April 1998.

[9] Black, M., and Jepson, A. D., "A probabilistic framework for matching temporal trajectories: CONDENSATION-based recognition of gestures and expressions", Proc. 5th European Conf. Computer Vision, pp. 909-924, 1998.

[10] Yunqiang Chen and Thomas S. Huang, "Model-based multi-object tracking in MAP framework", IAPR Workshop on Machine Vision and Applications, Tokyo, Japan. pp.455-458, 2000.